Journal of Applied Electrochemistry (2005) 35:273–278
DOI 10.1007/s10800-004-6773-8

The bromine electrode Part II: reaction kinetics at polycrystalline Pt

SERGIO FERRO, CHIARA ORSAN and ACHILLE DE BATTISTI*
Department of Chemistry, University of Ferrara, via L. Borsari 46, I-44100 Ferrara, Italy
*(*author for correspondence, e-mail: dbtcll@unife.it)*

Received 17 may 2004; accepted in revised form 12 November 2004

Key words: adsorbed intermediates, bromine electrode, electrosorption, platinum electrode, tests of mechanism

Abstract

The kinetics of bromide oxidation and Br_3^- reduction were studied at polycrystalline Pt electrodes in acidic media. The electrochemical behavior of equimolar Br_3^- and Br^- solutions was investigated, in a concentration range of the electroactive species between 0.1 and 1.0 M. E–log *j* plots did not exhibit linear segments, most probably because of extensive adsorption of bromine radicals. Further analysis supported the hypothesis of a Volmer–Tafel mechanism, with the chemical recombination step as rate determining. Electrosorption isotherms for Br radicals were found to be of the Frumkin type. The kinetics of Br_3^- reduction was controlled by the surface dissociation of the Br_2 molecules.

1. Introduction

Mechanistic studies of the kinetics of the bromine electrode have been carried out for essentially fundamental purposes [1–6], although dedicated studies [7] have also appeared in relation to Zn/Br_2 application [8, 9]. The number of such studies is limited, when compared to those focused on the more important chlorine evolution reaction (e.g. [10, 11] and references therein]. Thorough investigations have also been carried out in the presence of dilute (millimolar) Br^-/Br_2 solutions [1–5], or with only bromide ions in solution [6]. Due to the fact that electron transfer involving bromine species is fast, experiments reported in the literature were carried out at rotating disk electrodes [2, 5, 6], including impedance-based investigations [1, 3].

For Pt electrodes, Llopis and Vàzquez [1] proposed the electron transfer between the metal and bromine molecules to form Br_2^- ions (or a similar entity) as the rate determining step (r.d.s.), in both the cathodic and anodic directions. Substantial agreement exists among some of the subsequent work on the subject: Faita et al. [2], Cooper and Parsons [3] and also Rubinstein [4], in the case of an oxidized Pt surface, suggested bromide ions oxidation (leading to adsorbed $Br^{\cdot}$ species, 'Volmer step') as the r.d.s. in the anodic process. As reported in [4], *adsorbed* bromide ions are the reacting species (in the r.d.s.) at a 'reduced' electrode surface (i.e., an oxide-free Pt surface), in substantial agreement with Conway et al. [6] for the adsorption of Br^- with only a partial charge transfer (formation of $Br^{\delta-}$). The Br^- discharge was also found to be the r.d.s. at glassy carbon [5]. So far, only Conway and coworkers, in the most recent paper on the subject [6], have indicated chemical desorption ('Tafel step') as the r.d.s., in anodic bromine formation.

The present work reports bromine electrode kinetics at polycrystalline Pt, with the aim of elucidating both the anodic and the cathodic reaction mechanisms. Measurements were performed in the presence of both of the partners of the redox couple in equimolar concentrations.

2. Experimental

The electrochemical study was carried out using Autolab PGSTAT20 digital equipment; cyclic voltammetric measurements were performed at room temperature at a scan rate of 100 mV s^{-1}, making use of a SCANGEN module, for linear sweep generation. The chosen potential range was cycled using a step potential of 2 mV with repetition at least five times or until reproducible signals were obtained; in each case, the last cycle was recorded. Exchange current density values were obtained by recording quasi-steady polarization curves, at a scan rate of 0.1 mV s^{-1} and with a step potential of 0.15 mV, in a range ± 20 mV with respect to the open circuit potential (OCP), starting from the higher value and conditioning the electrode at the initial potential for 30 s. To explore the kinetics, especially under the high-overpotential approximation, polarization curves were recorded over a range ± 150 mV around the OCP, at a scan rate of 0.5 mV s^{-1} and with a step potential of 0.45 mV. Experiments, in both the low and high overpotential regions, were carried out under vigorous stirring by means of a magnetic stirrer.

All reagents were of special purity grade and solutions were prepared in milliQ water ($\rho > 18$ MΩ cm); extra pure NaBr (Riedel-de Haën), $HClO_4$ (70%, Aldrich), $NaClO_4$ monohydrate (Fluka) and Br_2 (≥99.5%, Carlo Erba, pack of 10×1 ml glass tubes) were used as received. A 2 M NaBr/1 M Br_2 (i.e., equimolar Br^-/Br_3^- solution) stock solution was prepared, adjusting the pH to a value of 2 with perchloric acid, and stored in the dark until utilization. Less concentrated solutions were obtained by dilution of the stock, by adding the appropriate amounts of $NaClO_4$ and $HClO_4$, to maintain a pH of 2 and a constant ionic strength (also equal to 2). A small platinum wire of 4.66 mm^2 real surface area, as determined by evaluation of the UPD hydrogen adsorption [12], a cylindrical platinum grid and a double-walled saturated calomel electrode (SCE), with an intermediate saturated $NaNO_3$ solution, were used as working, counter and reference electrode, respectively.

3. Results and discussion

Electrochemical measurements were carried out following the experimental set-up of Faita et al. [2], i.e., adjusting the pH of the different solutions to a value of 2. From the Pourbaix potential-pH equilibrium diagram for the bromine–water system [13], this choice should minimize possible interference of equilibria involving bromic acid. As expected, the Br_2/Br^- redox equilibrium does not depend on pH, but a subsequent reaction, possibly leading to the formation of hypobromous acid, is detectable by, e.g., cyclic voltammetry, as shown in Figure 1. The signals related to the latter electrochemical process show a pH dependence of about 50 mV per pH unit, which further supports the hypothesis of hypobromous acid formation. This reduces the polarization range within which the bromide oxidation kinetics can be studied, in the positive direction. Another interesting consideration concerns the data given in Figure 1; as reported in the first part of the present work [14], significant variations in surface concentration of Br-related species were measured at two different pH (1 M $HClO_4$ and 1 M $NaClO_4$ adjusted to a pH of 2), probably due to a screening effect exerted by O-related species, more readily formed at the latter pH. Referring to the Br_2/Br^- redox couple (centered at about 0.944 V_{SCE}), the higher peak currents, recorded at the less acidic pH, may be accounted for along the above lines.

The use of a stationary electrode was criticized in earlier work on the subject [2]. However, more recently, Conway et al. [6] showed that the recorded limiting current does not reflect any diffusion limitation of reacting species to the electrode surface. To verify this behavior, quasi-steady polarization curves at a Pt rotating disk electrode were carried out, in a solution containing 0.5 mol l^{-1} of both, Br^- and Br_3^-, at different rotation rates (500, 1500 and 3000 rpm). No difference was observed among the three runs, which appeared linear and with data points perfectly superimposed (figure not given). A subsequent trial was carried out, using a small (stationary) Pt wire, and similar results were obtained; therefore, the latter set-up was maintained for the rest of the study. A set of quasi-steady polarization curves, obtained at the Pt wire and recorded in solutions containing from 0.1 to 1 mol l^{-1} of Br^-/Br_3^-, is shown in Figure 2. In consideration of the relatively narrow range of explored overpotentials (±150 mV around the OCP), the attainment of a limiting current seems to occur only for the more diluted solution (0.1 M), and anyway only for η higher than 0.1 V. On the other hand, data in Figure 2 do not show the expected exponential dependence of j on η: curves appear anomalously linear, possibly as a result of the presence of an adlayer of Br-species [14] at the electrode surface, which increases the ohmic resistance of charge transfer.

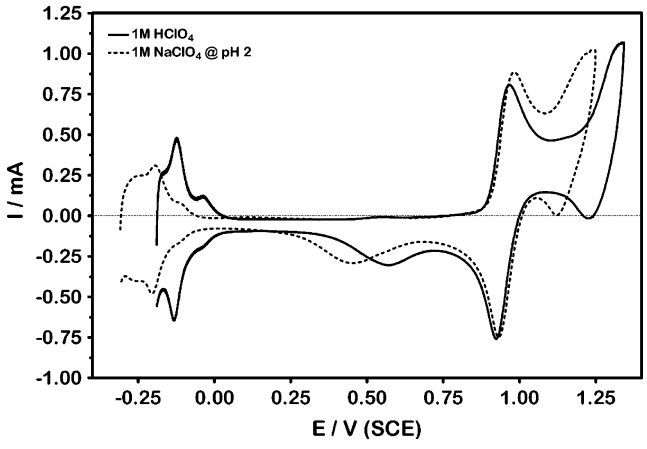

Fig. 1. Comparison of CV curves, obtained in 1 mM Br^-/Br_3^- solution, using 1 M $HClO_4$ (solid line) and 1 M $NaClO_4$ adjusted to a pH of 2 with perchloric acid (dotted line) as supporting electrolyte, respectively. Scan rate: 0.1 V s^{-1}.

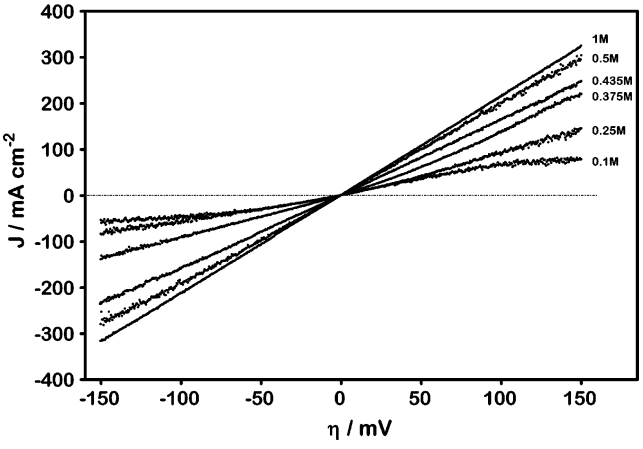

Fig. 2. Polarization curves (±150 mV with respect to each OCP) for the bromine electrode, recorded in x M Br^-/x M $Br_3^-/(2-2x)$ M $NaClO_4$/0.01 M $HClO_4$ (x from 0.1 to 1).

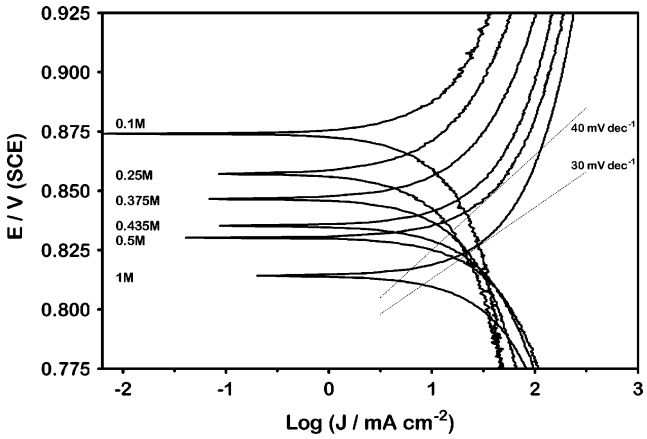

Fig. 3. Current–potential curves for the bromine electrode, recorded in x M Br^-/x M Br_3^-/(2−2x)M $NaClO_4$/0.01 M $HClO_4$ (x from 0.1 to 1). Theoretical Tafel slopes for the Volmer–Tafel (chemical recombination, 30 mV dec^{-1}) and Volmer–Heyrovsky (electrochemical recombination, 40 mV dec^{-1}) mechanisms are reported for comparison.

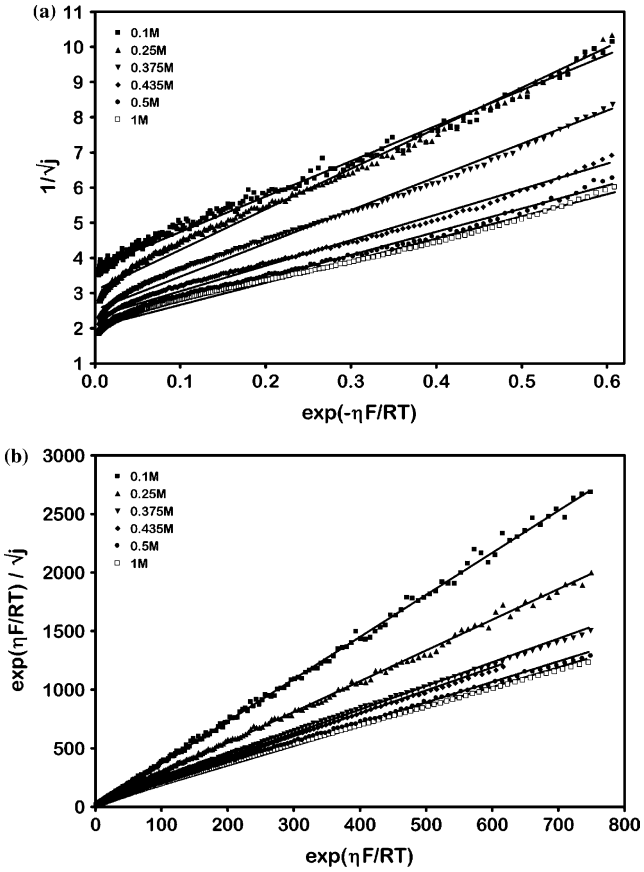

Fig. 4. Testing of the chemical-desorption-controlled mechanism for the bromide anodic oxidation, at different Br^-/Br_3^- concentrations. Equation 2a and 2b were used in (a) and (b), respectively; in both cases, a Langmuir-type isotherm was hypothesized for the Br coverage.

The processing of the same data, in terms of Tafel plots, is shown in Figure 3; the E–log j plots appear to be continuously curved, in harmony with the linear representations of Figure 2; analogous results were described also in [6], and justified through an activation-control due to the chemical desorption step. In the absence of the discriminating b value, further information on the mechanism of the anodic and cathodic reactions was obtained on the basis of the test equations already reported in the literature for the chlorine evolution reaction [6, 11, 15]. In the hypothesis of a Volmer–Tafel sequence of steps, with a kinetic control through the chemical recombination step, and using a Langmuir adsorption isotherm for the adsorbed intermediates, the following equation can be obtained:

$$j^{-1/2} = (2F\,k_2)^{-1/2} \times \frac{1 + K_1 C_{Br^-} \exp(F\eta/RT)}{K_1 C_{Br^-} \exp(F\eta/RT)} \quad (1)$$

which can be rearranged in two ways:

$$j^{-1/2} = (2F\,k_2)^{-1/2} + (2F\,k_2)^{-1/2} \times (K_1 C_{Br^-})^{-1} \times \exp(-F\eta/RT) \quad (2a)$$

or

$$\frac{\exp(F\eta/RT)}{j^{1/2}} = \frac{(2F\,k_2)^{-1/2}}{K_1 C_{Br^-}} + (2Fk_2)^{-1/2} \times \exp(F\eta/RT) \quad (2b)$$

In both cases, the left side quantity should be linear against the exponential term on the right side. Both types of plot are shown in Figure 4; exploiting their good linearity, estimations of k_2 (the kinetic constant of the Tafel step) and K_1 (the equilibrium constant of the Volmer step, $K_1 = k_1 / k_{-1}$) were obtained, and values are collected in Table 1.

In spite of the good results obtained under the Langmuir adsorption isotherm approximation, we also showed [14] that a Frumkin isotherm may be utilized, which seems more appropriate given that a significant coverage was found for the adsorbed intermediates (~60%; [14] and references therein). Accordingly, a substitution of isotherms can be made, even if the mathematical treatment requires a further approximation, that is, to consider a coverage of around 66% (as a result, $\ln(\theta/(1-\theta)) \approx \theta$); the current can thus be expressed with the following equation:

$$j = \frac{2F\,k_2(\ln K_1 C_{Br^-} + F\eta/RT)^2}{(1-2a)^2} \quad (3)$$

which can be rearranged to give the equation of a straight line, as follows:

$$(1-2a)\sqrt{j} = (2F\,k_2)^{-1/2} \ln K_1 C_{Br^-} + (2F\,k_2)^{1/2} \frac{F\eta}{RT} \quad (4)$$

Again, for recombination control, a linear relation should be obtained by plotting $(1–2a)\sqrt{j}$ vs the ratio $F\eta/RT$ (the proper value of a was taken from [14]). The resulting analysis is shown in Figure 5 (only η values in the range 0.025 to 0.1 V were considered, i.e., the

Table 1. Values of the kinetic constants K_1 and k_2 for the chemical-recombination-controlled bromide oxidation, at different solution compositions and for the considered adsorption isotherms.

	0.1 M	0.25 M	0.375 M	0.435 M	0.5 M	1 M
Langmuir isotherm (EQ. 2a)						
Goodness of fit (R^2)	0.9911	0.9897	0.987	0.9875	0.9871	0.9875
K_1	3.70	1.07	0.71	0.74	0.65	0.32
k_2 ($\times 10^{-5}$)	7.20	4.92	3.31	2.82	2.32	2.16
Langmuir isotherm (EQ. 2b)						
Goodness of fit (R^2)	0.9992	0.999	0.9985	0.9987	0.9986	0.9987
K_1	2.96	0.45	0.22	0.25	0.19	0.10
k_2 ($\times 10^{-5}$)	6.69	3.57	2.11	1.98	1.59	1.46
Frumkin isotherm (EQ. 4)						
Goodness of fit (R^2)	0.9739	0.9929	0.9957	0.9922	0.9908	0.9928
K_1	137.6	20.8	14.0	21.8	19.2	9.7
k_2 ($\times 10^{-10}$)	4.16	7.84	11.46	11.32	13.67	14.70

potential interval in which the high overpotential approximation of the Butler–Volmer equation should be respected). Although a poorer linearity was obtained, compared with Figure 4, an analysis giving the k_2 and K_1 values was carried out, whose results are shown in Table 1. It is interesting to observe that both K_1 and k_2 differ in orders of magnitude, depending on the assumed form of the isotherm. The Langmuir isotherm is appropriate at very low coverage, while the Frumkin one, which accounts for lateral interactions (both attractive and repulsive), has a wider range of application ($0.1 < \theta < 0.9$); consequently, it is not surprising to observe what follows:

$$K_{1,\text{Frumkin}} > K_{1,\text{Langmuir}} \text{ while } k_{2,\text{Frumkin}} << k_{2,\text{Langmuir}}$$

Bearing in mind the meaning of K_1 and k_2 (which are measured in $cm^3\ mol^{-1}$ and $mol\ s^{-1}\ cm^{-2}$, respectively), high θ values are attained if the 'Volmer step' is shifted toward the formation of the reaction intermediates ($K_{1,\text{Frumkin}} > K_{1,\text{Langmuir}}$) and the subsequent 'Tafel step' has a slow rate constant ($k_{2,\text{Frumkin}} < < k_{2,\text{Langmuir}}$). Both results comply with the behavior of data in Figure 2, supporting the idea that the electrode surface is covered by a layer of adsorbed Br· radicals.

Further processing was attempted, taking into account the analytical relation proposed by Tilak and Conway [16], which links the experimentally measurable reaction order ($\mathscr{R}$), the kinetically-significant surface reaction order ($\mathscr{R}_s$) and the adsorption isotherm function. In the case of the Frumkin isotherm, one has:

$$\left(\frac{\partial \ln j}{\partial \ln c}\right)_{E,T} = \left(\frac{\partial \ln j}{\partial \ln \theta}\right)_{E,T} \times \left(\frac{\partial \ln \theta}{\partial \ln c}\right)_{E,T}$$
$$\Rightarrow \mathscr{R} = \mathscr{R}_S \times \frac{1-\theta}{1+2a\theta-2a\theta^2} \qquad (5)$$

Considering the Volmer–Tafel mechanism, with rate control by chemical desorption, the current can be written as follows:

$$j = 2F\,k_2\theta_{\text{Br}\cdot}^2 \qquad (6)$$

with $\mathscr{R}_s = 2$. On the other hand, once a proper potential value is chosen in Figure 3, the value of $\mathscr{R}$

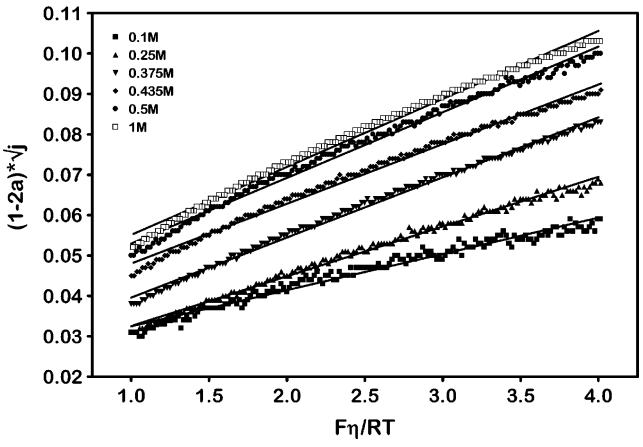

Fig. 5. Testing of the chemical-desorption-controlled mechanism for the bromide anodic oxidation, based on a Frumkin-type adsorption isotherm; η values were restricted to the range from 0.025 to 0.1 V (high-overpotential approximation).

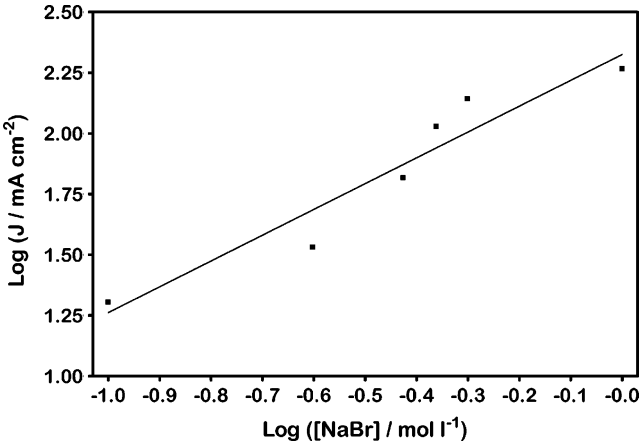

Fig. 6. Dependence of the reaction rate for the bromide oxidation on the Br^- concentration; current values were taken at 0.9 V_{SCE}.

(≈1.06) was estimated from the slope of a bilogarithmic j vs c plot (Figure 6), referring to a potential of 0.9 V_{SCE}, corresponding to overpotential values all in the range of linearity of Figure 5. Knowing both $\mathscr{R}$ and $\mathscr{R}_s$, the coverage was determined through Equation 5, leading to a θ value of 0.37.

This estimation is significantly lower than the value previously hypothesized ($\theta \approx 0.66$) to test the chemical recombination mechanism. While the latter was assumed for mathematical purposes (in order to simplify the equation and to carry out the test), the former suggests that lower $\theta_{Br\cdot}$ values may be attained at anodic overpotentials higher than under the CV conditions reported in [14]. Such a result is not surprising, considering that the coverage is related to the electrode potential (through the electrosorption isotherm), and it also depends on the concomitant presence of O-related species at the Pt electrode surface.

The above analysis could be criticized, because the evaluation of a reaction order requires carrying out measurements at constant composition, varying only one reactant concentration. In the present case, a chemical equilibrium exists between the species present in solution:

$$Br^- + Br_2 \rightleftharpoons Br_3^- \tag{7}$$

the chemical constant being $K_{eq} = [Br_3^-]/[Br^-]\,[Br_2]$. Since the solution composition was chosen in such a way that $[Br_3^-] \approx [Br^-]$ (also for the different solutions), the concentration of the remaining species is determined by the chemical constant and, in particular, $[Br_2] \approx 1/K_{eq}$. Accordingly, if the latter is effectively invariant, the reaction order analysis cannot be considered erroneous; however, a verification of the above approximation will be given in a subsequent section of this paper.

Concerning the cathodic process (reduction of Br_2 or Br_3^- to Br^-), data in Figures 2 and 3 show that, again, no definite Tafel linearity can be recognized; as a result, the mechanism of the reaction was investigated through the same approach previously applied for the anodic process. The different possibilities are summarized in the following sequence of steps:

$$\begin{aligned}
&\text{(i)} \quad S + Br_3^- \rightarrow S - Br_2 + Br^- \\
&\text{(ii)} \quad S - Br_2 + e \rightarrow S - Br^\bullet + Br^- \\
&\text{(iii)} \quad S - Br_2 + S \rightarrow 2S - Br^\bullet \\
&\text{(iv)} \quad S - Br^\bullet + e \rightarrow S + Br^-
\end{aligned} \tag{8}$$

Step (i) is representative of the polybromide ion dissociation, which produces a physisorbed bromine molecule and a bromide ion; such a step should be considered to account for the considerable solubility of bromine, which is due to the formation of Br_3^- ions. The mechanism of bromine reduction could be further described by the occurrence of step (ii) (or, alternatively, step (iii) and (iv); if the latter is rate-determining, the current would be dependent on the overpotential (electrochemical step). An analogous result would be obtained assuming step (ii) as r.d.s.. The test of the mechanism excluded both hypotheses. On the other hand, considering the very good symmetry of curves in Figures 2 and 3, a 'symmetry' should also be expected for the reaction mechanism. It therefore seems reasonable to assume step (iii) as rate-determining in the cathodic direction, in agreement with the chemical recombination control found for the anodic process. The similarity also extends to the presence of adsorbed Br·, due to the dissociative adsorption of Br_2 (details were given in [14]); such adlayer is plausibly responsible for the lack of any linearity in Figure 3, as already discussed when the anodic process was analyzed.

A final examination was performed, on the basis of the data recorded under low-overpotential approximation; linear j/η plots were obtained, as shown in Figure 7, allowing the determination of the exchange current density for the different concentration conditions (values are collected in Table 2). In addition, the validity of the approximation previously used for the reaction order analysis (Equation 7 and related statements) could be verified, testing the equation:

$$\begin{aligned}
\varepsilon_0 &= E_0 + \frac{RT}{F}\ln\frac{[Br_2]^{1/2}}{[Br^-]} \\
&= E_0 + \frac{RT}{F}\ln\frac{[Br_3^-]^{1/2}}{[Br^-]^{3/2}\cdot K_{eq}^{1/2}} \\
&\approx E_0 + \frac{RT}{F}\ln\frac{1}{[Br^-]\cdot K_{eq}^{1/2}}
\end{aligned} \tag{9}$$

obtained based on the Nernst equation and assuming $[Br_3^-] \approx [Br^-]$. The linearity of the plot ε_0 against the logarithm of $[Br^-]$, with a slope of −1, eventually confirmed the applied approximation.

4. Conclusions

The anodic oxidation of bromide at a polycrystalline Pt electrode takes place through a Volmer–Tafel

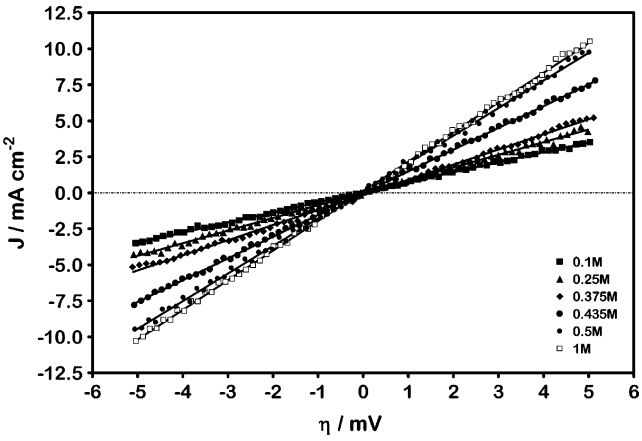

Fig. 7. Polarization curves (low-overpotential approximation) for the bromine electrode, recorded in x M Br^-/x M Br_3^-/(2−2x) M $NaClO_4$/0.01 M $HClO_4$ (x from 0.1 to 1).

Table 2. Values of exchange current density and equilibrium potential as a function of the solution composition

Br^-/Br_3^- concentration/M	$dj/d\eta$	j_0/mA cm^{-2}	ε_0/V vs SCE
0.1	0.698 (3)	17.9	0.8740
0.25	0.877 (5)	22.5	0.8575
0.375	1.050 (6)	26.9	0.8470
0.435	1.510 (4)	38.7	0.8352
0.5	1.916 (8)	49.2	0.8302
1	2.058 (7)	52.8	0.8143

mechanism, its rate being controlled by the chemical desorption step, as reported for Cl^- oxidation (e.g. [17] and literature therein). However, while in the latter case the coverage by intermediate radicals is not very high, and Tafel linearity is found at most of the electrode materials, in the case of Br^- oxidation, $\theta_{Br\cdot}$ is close to unity across the whole polarization window of Pt. As discussed in the first part of this investigation [14], only the onset of oxygen adsorption, in the potential region where Br_2 formation takes place, causes a decrease in $\theta_{Br\cdot}$ and changes in the parameters of the electrosorption isotherm, which, in turn, is reflected in the kinetics of bromide oxidation and bromine reduction. The co-existence of bromine and oxygen radicals at the electrode surface may allow the kinetic conditions for further reactions, eventually leading to oxy-anionic species. Again, a parallel with the chlorine evolution mechanisms, involving oxy-chloro surface complexes, may be suggested. Referring to the cathodic reaction, the present data suggest the dissociative adsorption of bromine as the r.d.s.. However, while the interactions with the electrode surface favor a spontaneous adsorption of Br· species, the stabilization of radicals is possibly strong enough to prevent the subsequent desorptive reduction: as a result, the charge transfer reaction takes place through the adlayer instead of happening on the bare Pt surface. The present conclusions are fully supported by data in [14], and additional concurrence may be found in the literature concerning the adsorption of Br_2 under ultra-high vacuum conditions. Further research is planned to describe the influence of the nature of the electrode material on the kinetics of bromide oxidation and bromine reduction.

References

1. J. Llopis and M. Vàzquez, *Electrochim. Acta* **6** (1962) 177.
2. G. Faita, G. Fiori and T. Mussini, *Electrochim. Acta* **13** (1968) 1765.
3. W.D. Cooper and R. Parsons, *Trans. Faraday Soc.* **66** (1970) 1698.
4. I. Rubinstein, *J. Phys. Chem.* **85** (1981) 1899.
5. M. Mastragostino and C. Gramellini, *Electrochim. Acta* **30** (1985) 373.
6. B.E. Conway, Y. Phillips and S.Y. Qian, *J. Chem. Soc. Faraday Trans.* **91** (1995) 283.
7. P.K. Adanuvor, R.E. White and S.E. Lorimer, *J. Electrochem. Soc.* **134** (1987) 1450.
8. C.S. Bradley, *US Patent n. 312,802* (1885).
9. G. Tomazic, *US Patent n. 2003/0,113,615* (2003).
10. S. Ferro, A. De Battisti, I. Duo, Ch. Comninellis, W. Haenni and A. Perret, *J. Electrochem. Soc.* **147** (2000) 2614.
11. S. Ferro and A. De Battisti, *J. Phys. Chem. B* **106** (2002) 2249.
12. J.M. Doña Rodríguez, J.A. Herrera Melián and J. Pérez Peña, *J. Chem. Educ.* **77** (2000) 1195.
13. M. Pourbaix, 'Atlas of electrochemical equilibria in aqueous solutions, National Association of Corrosion Engineers' (Houston, Texas, USA, 1974) pp. 604–613.
14. S. Ferro and A. De Battisti, *J. Appl. Electrochem.* **34** (2004) 981.
15. B.E. Conway and D.M. Novak, *J. Electroanal. Chem.* **99** (1979) 133.
16. B.V. Tilak and B.E. Conway, *Electrochim. Acta* **37** (1992) 51.
17. D.M. Novak, B.V. Tilak and B.E. Conway, *in* B.E. Conway and J. O'M Bockris (Eds), 'Modern Aspects of Electrochemistry',Vol. 14 (Plenum Press, New York, 1982) p. 195.